Proc. Indian natn. Sci. Acad., **62**, A, No. 6, 1996, pp. 461-473.

REVIEW ARTICLE

NEAR-UNSTABLE STARS : THE YELLOW-WHITE HYPERGIANTS

CORNELIS DE JAGER

SRON Laboratory for Space Research; Sorbonnelaan 2, 3584 *CA Utrecht, The Netherlands*

(*Received* 4 *January* 1996; *Accepted* 23 *March* 1996)

The yellow-white hypergiants are stars of extreme luminosites (10^5 to 10^6 times the Sun) with effective temperatures between 4000 and 10000 K. The effective photospheric acceleration of gravity is of the order of 0.1 to 3 cm s^{-2}. Atmospheric abundances and mass determinations suggest that the stars are evolved objects, moving blueward in their evolution. Three well-studied objects are described (Rho Cas, HR 8752, and HD33579).

Methods of spectroscopic diagnosis allows for a determination of the various accelerations acting on the photospheric gas and thus make possible a determination of the stellar mass. The observed photospheric small-scale motion field is ascribed to shock waves with largest wavelengths 2.5 times the atmospheric density scale height, and moving upward through the photosphere.

In the Hertzsprung-Russell diagram the yellow hypergiants are situated at the low-temperature side of a region of atmospheric instability : the Yellow Evolutionary Void. This suggests a relation: since these stars are evolving in the HR diagram from the red supergiant region towards the blue, it is natural that the atmospheres become unstable, with a consequent increased rate of mass loss, when the star is nearing the Void. The subsequent ejection of an optically thick shell may also explain the occurrence of extended periods during which the stars have reduced effective temperatures.

Key Words: Near-Unstable Stars; Yellow-White Hypergiants; Atmospheric Diagnostics; Photospheric Acceleration; Stellar Mass Determination; Yellow Evolutionary Void.

The Yellow-White Hypergiants

Hypergiants are stars with more extreme spectral luminosity characteristics than normal supergiants of luminosity class Ia; their luminosity class is usually written as Ia^+.

The yellow hypergiants are stars with average effective ('surface') temperatures of 7000 K (range: $\pm$ 3000 K), average luminosities of 4×10^5 times the solar value (range $\pm 3 \times 10^5$). The value for the atmospheric acceleration is about 0.1 to 3 cm s^{-2}. The white hypergiants have similar characteristics, but their temperatures are higher, around 10000 K. There is about half a dozen resonably well-studied yellow-white hypergiants and a similar number of less well studied objects; the latter are for the most part found in other extragalactic systems than ours.

Their positions in the Hertzsprung-Russel diagram are shown by open circles in Fig. 1. It shows the large luminosities and the yellow-white colours. In

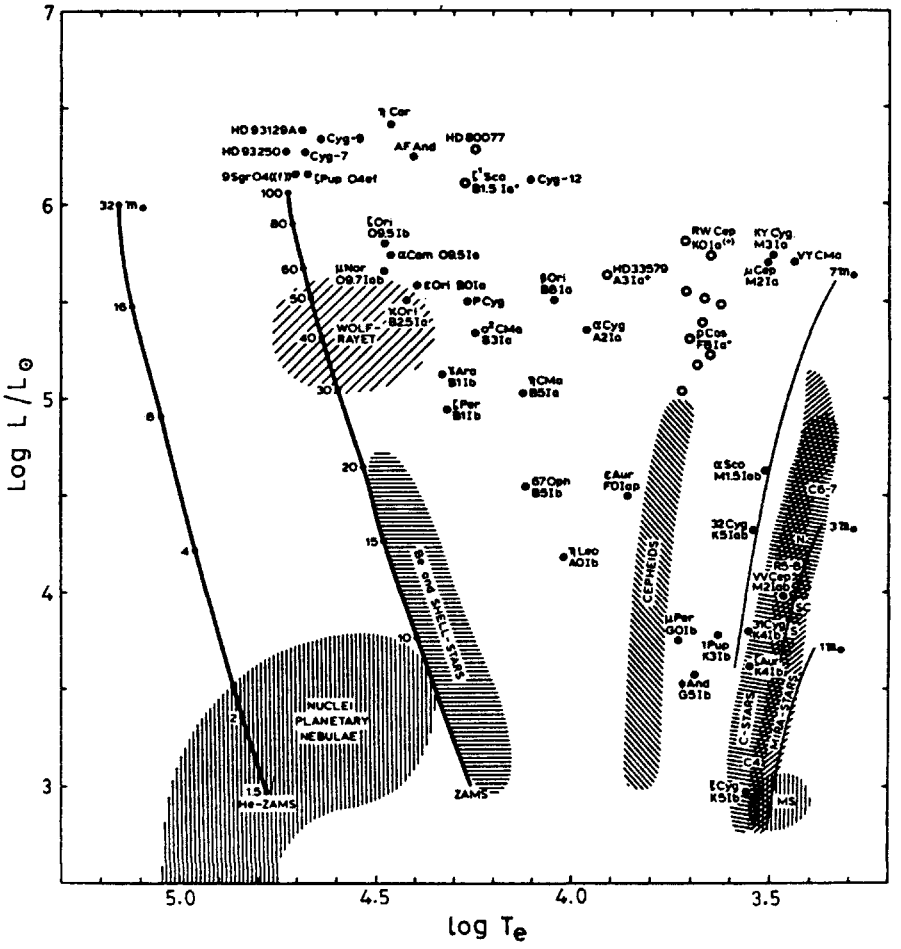

Fig. 1 Upper part of the Hertzsprung-Russell diagram; hypergiants are indicated by open circles

Table I we list some properties of three of the best studied yellow and white hypergiants: HD33579[1]; HD217476[2] and HD224014. These are the objects specially described in this paper.

The stellar masses in the above table were kindly calculated by Dr. Hans Nieuwenhuijzen, using observed values for $T_{\rm eff}$, $L/L_{\odot}$, $g_{\rm eff}$, ζ_{μ}, $T(\tau_{\rm av})$ and M, with a method described in the present section 3 and in Nieuwenhuijzen and de Jager[4].

The stars show various signs of instability. Their luminosity may vary semi-regularly with quasi-periods of the order of months to a year, and small amplitudes, of the order of 0.2 magnitudes. It happens occasionally that their spectral types vary considerably, with excursions to lower temperatures. This process covers periods of the order of several years to tens of years. An example of this latter phenomenon is presented by the star HR8752. Around 1950, the spectrum was G0 Ia corresponding to an effective temperature of 5800 K. In later years it cooled down slowly, to reach the spectral type K2-K5 Ia in

Table I

Three well-studied yellow-white hypergiants

HD	Other name	Spectrum	T_{eff} (K)	$\log(L/L_{\odot})$	$M/M_{\odot}$
33579	—	A3 Ia$^+$	8000	5.7	46
217476	HR8752	G0-G5 Ia$^+$	4550	5.3	25
224014	ρ Cas	F8 Ia$^+$	7190	5.7	32

Table II

Variation of T_{eff} of HR8752; Nieuwenhuijzen, Lobel and de Jager, in prep

Year	T_{eff}(K)
1973	4900
1978	5600
1984	4550

1973, which corresponds to a photospheric temperature of about 4000 K. Thereafter, the spectrum returned to an earlier type again, and in 1978 it was described as G0 Ia$^+$ to G5 Ia$^+$ (5300 K). This rapid cooling, followed by a slower recovery to the previous higher value, is ascribed to 'veiling' of the atmosphere by large amounts of ejected gas, which causes the effective photospheric temperature, as well as the value of the effective acceleration, to decrease. This phenomenon has recently been studied by using quantitative spectroscopic data. Nieuwenhuijzen *et al.*[2] on the basis of spectral diagnostics of a number of high-resolution spectra, determined the effective temperature of the star and found the long-term variations shown in Table II. Differences with values given above are due to the fact that the above first mentioned temperatures are derived from the visual appearance of spectra which is less certain than values obtained from quantitative spectral line diagnostics. Remarkable is the occasional drop in the effective temperature in 1984. We ascribe it to large mass ejections. The reduction of the effective acceleration which occurs at the same time is in agreement with the picture of an atmosphere losing an optically thick shell of mass by a general outstreaming motion.

The star ρ-Cas had a K-type spectrum before 1930, but in 1943 it was F8 IA, which is the value commonly accepted. However, during the years 1946-1947 the visual magnitude decreased by about 1.5 mag and during several months during 1947 the star showed M-characteristics. At present, the effective temperature is 7190 K, which would correspond with a spectral type F0, which is hot as compared to the commonly accepted 'average' value (F8)[3].

Atmospheric Diagnostics

In the last few years our group at Utrecht has tried to improve methods for atmospheric diagnostics[1,3,7].

Input data for such studies are a sufficiently large number of equivalent widths (W_{obs}) of spectral lines, covering a good range of values (from weak to middle-strong lines). Some 50 W_{obs}-values appears to be an absolute minimum for a reliable study. More are preferable. We also need reliable atomic data for these lines. The atomic oscilator strengths are the weakest element in this procedure. The W_{obs}-values are then compared with calculated equivalent widths W_{cal} for a number of selected photospheric models chosen in a suitable range of values of four photospheric parameters, *viz.* the effective temperature T_{eff}, the photospheric acceleration g_{eff}, the heavy elements abundances $Z/Z_{\odot}$, and the average value of the line-of-sight small-scale velocity component ζ_{μ}. The observed and calculated W-values are then compared in a minimum χ^2 method till agreement is reached between (a) the scatter of data expected on the basis of errors in the measured W-values and in the gf-data, and (b) the scatter resulting from the best fit. The analysis then yields values for the four photospheric parameters listed above.

We make two additional remarks. The interpretation of the derived values for ζ_{μ} is a delicate problem, cf. the next Section. An essential other element of the analysis is that each spectral line has its own *depth of formation.* The photospheric contribution to a line originates from a fairly extended range of photospheric depths for which an average optical depth value τ_{av} can be determined. This value is not necessarily the same for each line. A suitable *general average depth of line formation* for the whole set of lines appears to be $\tau_{Ross} = 0.03$.

Effective Acceleration and Stellar Mass Determination

In current astrophysical literature one sometimes meets values for stellar masses derived on the basis of the g_{eff}-values as obtained in the above or in related ways. It is then implicitely (but erroneously) assumed that the value of the acceleration is equal to the Newtonian (gravitational) value. Since the effective temperature and absolute luminosity yield the stellar radius, the stellar mass can then be derived straightforwardly. The error is the implicite assumption, because especially for very luminous stars the effective acceleration can be smaller than the Newtonian value by factors as large as 5, with consequently the same relative errors in the derived masses.

Nieuwenhuijzen and de Jager[4,8] complied with this problem in the following way. They restrict themselves to the average depth of the line formation, being the reference level to which the observations refer. For that depth the temperature, the effective acceleration and the small-scale velocity component are known from the spectral analysis, next to two general stellar data : the effective temperature and the luminosity. Unknowns in the system are a number of data at the reference level : the pressure, the Newtonian acceleration, and the radiative shock-wave and stellar wind acceleration. By an iterative treatment the equation is solved, yielding among other things the Newtonian acceleration. This data allows for the mass determination, which we consider more reliable

than previously determined values (with the evident exception of masses determined from binary motion, but such cases do not exist for hypergiants). The mass-values in Table I are based on such a determination. An important conclusion from these results is that HR8752 and ρ Cas are indeed blueward evolving stars, while HD33579 is younger and evolving redward. This result is in line with abundance determination, and it also explains that HD33579 can be situated inside the yellow Evolutionary void (see the last but one section).

Atmospheric Dynamics; Small-scale Motion Field

Observations of the atmospheric motion field of any star are usually restricted to two spectrally observable parameters: the *micro-* and *macroturbulent velocity components*. The first kind of motions influences equivalent widths of medium strong spectral lines, and the second influence spectral line *widths* while leaving their *equivalent widths* unchanged. Conventionally, microturbulence is referred to as the 'small-scale' motion field, typically involving length-scales along the line of sight, that are small as compared with the mean free path of a photon, and the reverse applies to macroturbulence. Clearly, micro- and macroturbulence are asymptotic cases of a full motion field, since in actual stellar atmospheres we are virtually always dealing with a *spectrum of motions*, involving a continuous range of length scales. This spectrum can be Fourier-decomposed, at least in principle; this procedure introduces the wavelengths L or, alternatively, the wavenumbers $k = 2\pi/L$ occurring in the motion field. Following Kolmogoroff we conventionally assume that non-zero kinetic energies exist only for a restricted range of L values, starting from a largest value L_0, where kinetic energy is assumed to be fed into the motion field, till a smallest one L_1 below which energy is dissipated by viscosity.

As can be understood, not only the motions with the asymptotic values contribute to the observed microturbulent increase of the equivalent width or to the macroturbulent line broadening; the intermediate length scales contribute to both, and intuitively it will be felt that motions at relatively small wavelengths contribute most to microturbulence and that the relative contribution decreases for increasing wavelengths. The reverse applies to macroturbulence. Thus the notions micro- and macroturbulent filter functions $F_\mu(L)$ or $F_\mu(k)$ and $F_M(L)$ or $F_M(k)$ can be defined[9,10]. Here, F is the fraction of the kinetic energy of the motion field for a certain line-of-sight wavelength L or line-of-sight wave number k, that either contributes to the microturbulent increase of equivalent width or to the macroturbulent line broadening (Fig. 2).

On the basis of the above considerations, using observational data on micro- and macroturbulence of a number of super- and hypergiants, De Jager *et al.*[11] derived values for the longest wavelength in the spectrum of turbulence of these stars. A typical value appears to be 2.5 H_ρ, where H_ρ is the density scale height of the atmosphere.

Motions in Hypergiant Atmospheres

In non-magnetic stellar atmospheres two motion forms can exist in stellar atmospheres, depending on the restoring force acting on an imposed deviation from the stable situation. For *pressure waves* the restoring force is gas-pressure

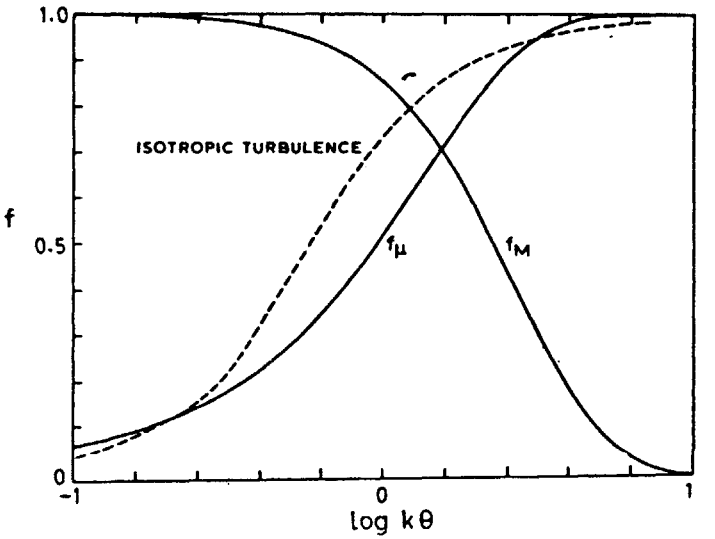

Fig. 2 Micro- and macroturbulent filter functions. The abscissa is dimensionless; k is the wavenumber and $\theta = dz/d\log\tau$, the optical scale height, with z = geometrical and τ = optical depth. The dashed line is due to Durrant[14] and the solid ones to de Jager and Verma[10]

and the properties of *gravity waves* are defined by gravitation as a restoring force. In a magnetic environment Alfvén waves can occur; their restoring force is the magnetic tension. But since magnetic fields have so far not been measured in cool hypergiants, we neglect that motion form.

The properties of the motions that are possible in stellar atmospheres are well demonstrated by a diagnostic (k, ω) or (P, L) diagram, in which the periods P or the frequencies ω of the possible waves are plotted against their wavelengths L or wavenumbers k. For small adiabatic disturbances in a non-viscous and isothermal gas in hydrostatic equilibrium the dispersion relation is given by

$$D=(\omega^2-N_{ac}^2)\omega^2/s^2-\omega^2k^2+N_{BV}^2k^2\sin\theta^2=0, \quad \ldots (1)$$

where θ is the angle between the vertical and the sound vector k. Further, N_{ac} is the acoustic cut-off frequency

$$N_{ac}=s_{ac}/2H=\gamma g/2s_{ac} \quad \ldots (2)$$

with s_{ac} = the speed of sound for pressure waves, H = pressure scale height, γ = the ratio of specific heats, g = the effective acceleration in the stellar atmosphere (being the algebraic sum of all in- and outward directed accelerations). Finally, N_{BV} is the Brunt-Väisälä frequency :

$$N_{BV}=(\gamma-1)^{1/2}\,g/s_{ac}. \quad \ldots (3)$$

For purely vertical waves $\theta=0$, hence only pressure waves can propagate strictly vertically; in eq. (1) the term with N_{BV} then drops out. Gravity waves

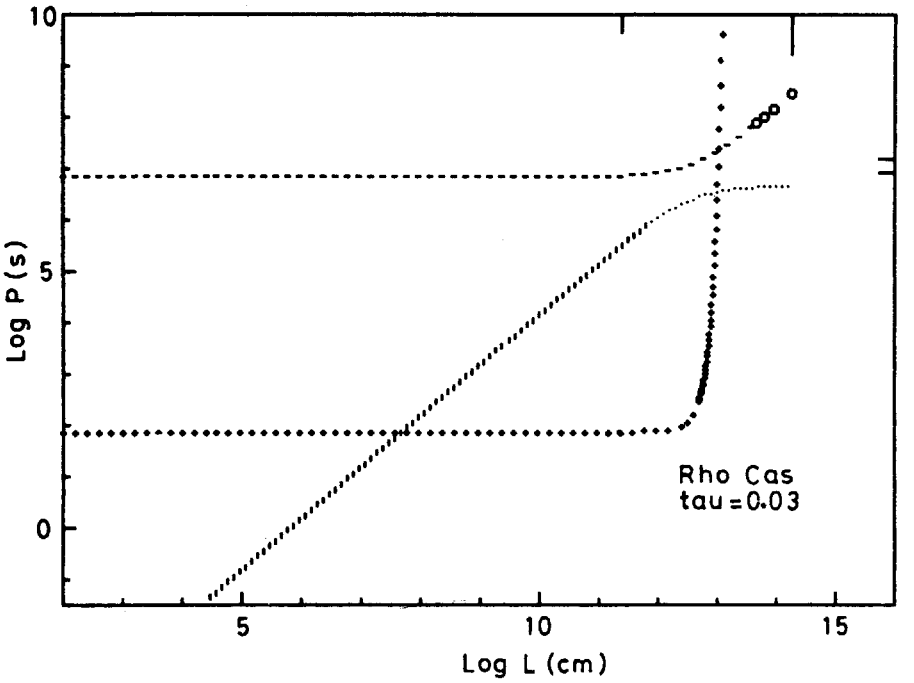

Fig. 3 Diagnostic diagram for atmospheric motions in ρ Cas, showing (short horizontal bars:) gravity waves; (short vertical bars:) pressure waves; (plusses:) thermal cut-off line. The four little circles on the gravity wave line give the P, L-values for waves with wavelengths equal to 1, 1/2, 1/3 and 1/4 times the stellar circumference. The dotted part of the pressure wave line gives the P, L-area where $L > 2.5\ H_\rho$ for which no pressure waves are expected. Short tic marks along the upper abscissa give the photospheric scale height (the shortest) and the stellar circumference; the tic mark(s) along the right-hand ordinate give the observed quasi-period(s) of stellar variability

apparently propagate mainly in the horizontal direction; they do not propagate strictly vertically.

Figure 3 shows a diagnostic P, L diagram for the average level of line formation $\tau_{av} = 0.03$ in the star ρ Cas. Here, the P, L-area where pressure waves can occur reduces to a thin line, drawn by short vertical bars in the diagram. This line covers the solution of eq. (1) for all possible θ-values. Only in the bending area, where P_{press} approaches P_{ac}, the area broadens somewhat, but even there less than the 'thickness' of the line.

The situation is different for gravity waves; these are possible in the whole area above the line drawn as short horizontal bars in the figure. The line itself corresponds to the case $\theta = 0$ (horizontal propagation). Infinitely long periods correspond to $\theta = \pi/2$.

Although Fig. 3 suggest that wave are possible for all possible wavelengths this is not the case for gravity waves. First, there is the upper wavelength limit set by the stellar circumference $2\pi R$, which defines the longest possible wavelength for gravity waves. But next there is the effect of radiative damping, which occurs because of the radiative interaction between hot and cool parts

of the waves, and which reduces the existence of waves with short periods, for which radiative interaction and consequent temperature equalization is strong. The radiative damping depends on the absorbing properties of the gas involved[12].

For very extended stellar atmospheres and long wavelengths, both cases applying to the cool hypergiants, an additional effect must be incorporated: atmospheric curvature reduces the radiative interaction of parts of the waves that are below each other's horizon, and it thus reduces damping for the longest wavelengths, a case considered by de Jager *et al.*[11], to which we refer for details of the mathematics. The effect is that waves with very long wavelengths are not damped. The limit of the *P*, *L*-area where radiative damping is still important is given by the line drawn as plusses. The curvature effect therefore allows for the existence of long waves that would be damped in a flat plan-parallel atmosphere.

This restriction does not apply to pressure waves, since these are expected to move chiefly into a vertical direction. As stated in the previous section these appear to exist for wavelengths below about 2.5 H_ρ. It is for that reason that we have drawn the pressure wave line in Fig. 3 as a dotted line for 'wavelengths' (actually: distances between successive shocks) longer than 2.5 H_ρ.

The figure appears to show that in the case of this star gravity waves are only possible for wavelengths between log $L=13$ (10^8 km) and the stellar circumference (see the longer tic mark along the upper abscissa). Circles along the gravity-wave line mark the period-wavelengths relations for waves with wavelengths of 1, 1/2, 1/3 and 1/4 times the stellar circumference. The tick mark along the right hand ordinate indicates the observed 'quasi-period' of the stellar variation, i.e., the main period in a periodogram of stellar brightness variations. In this particular case this period agrees fairly well with the horizontal part of the gravity wave line, which is the Brunt-Väisälä period. This comparison also shows that the very long periods are not dominantly present in the stellar brightness variations. In other words: the star pulsates mainly in non-radial overtones, in which various frequencies are possible. This gives rise to a rather complex looking lightcurve, as is indeed observed.

In Figs. 4 and 5 we show the diagnostic *P*, *L*-diagrams for the two other stars. HD33579 (Fig. 4) is a case contrasting with ρ Cas. The observations show a smooth lightcurve, practically without overtones, in which a quasi-period of 100 days is observed[5,6]. The diagnostic diagram confirms this: only gravity waves with wavelengths longer than $2\pi R/3$ and periods above ~ 3 yr are possible. The observed quasi-period of 100d corresponds[5,6] with shock-waves with wavelengths of 2.5 H_r, again in agreement with our earlier finding[11]. Since this period apparently dominates, the shocks seem to involve a fairly large part of the stellar surface.

For HR8752 (Fig. 5) the situation is fairly similar to that of ρ Cas.

The Yellow Evolutionary Void

Section 3 described a method to find the stellar mass M_* from given data: L_*, $T_{\rm eff}$, $g_{\rm eff}$, ζ_μ, $T(\tau_{\rm av})$ and M, where $\tau_{\rm av}$ is the average photospheric depth of forma-

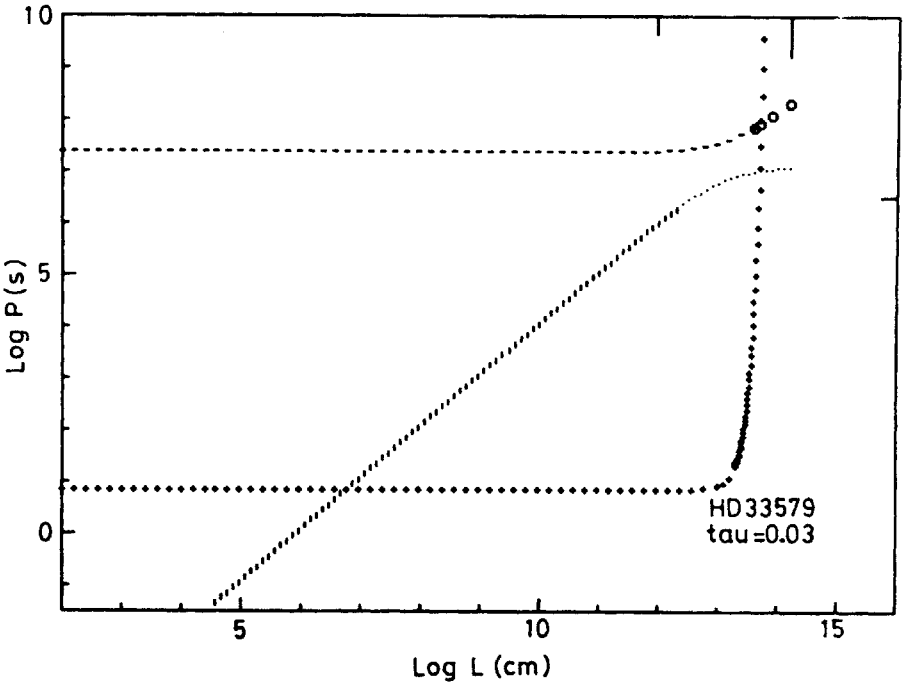

Fig. 4 Diagnostic diagram for HD33579

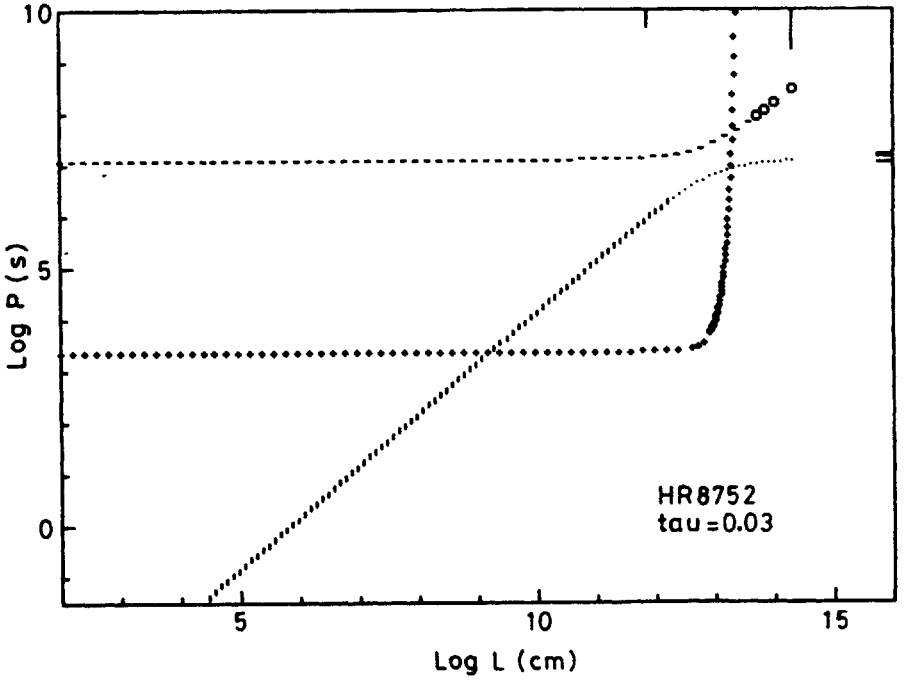

Fig. 5 Diagnostic diagram for HR 8752

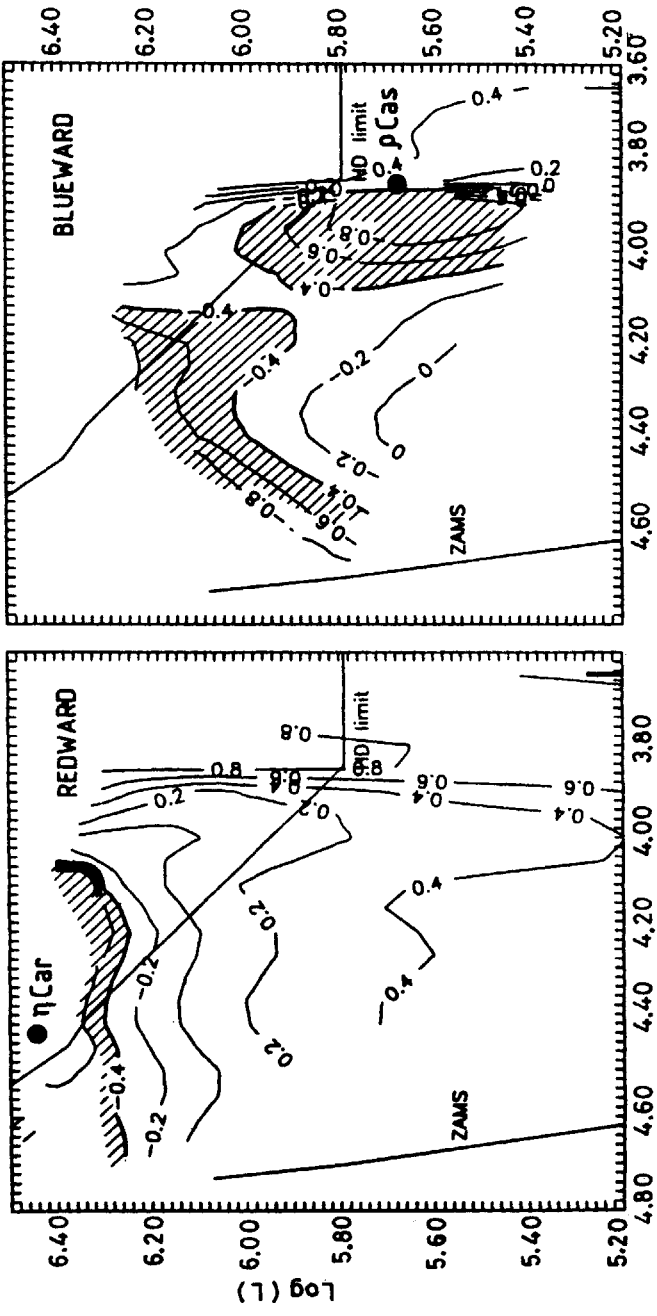

Fig. 6 Instability areas in the HR diagram. *Left*: redward evolution; *right*: blueward evolution. In the hatched areas stars have unstable photospheres

tion of the spectral lines. The problem will now be reversed by assuming M_* known for any place in the Hertzsprung-Russel diagram (defined by L_* and T_{eff}), by taking ζ_μ from a statistical relation between ζ_μ and $L/L_\odot$, by assuming the effective temperature is reached at the optical depth $\tau = 0.67$, and thus deriving g_{eff} for any point int he Hertzsprung-Russel diagram[4]. The values of M_* are taken from evolution calculations. In this connection we have to distinguish between stars moving redward in the HR-diagram, and the more evolved stars, which have passed the 'red turning point' of stellar evolution and are moving blueward. The latter have considerably smaller masses than the former because of the continuous mass loss of the stars.

This yields the following results[8] :

For stars evolving redward (left hand diagram of Fig. 6) there is a smooth and monotonous distribution of g_{eff}-values over the HR diagram, the values decreasing towards lower temperatures and higher luminosities. The values labeling these lines give the log of the ratio between the upward pulsational and downward effective acceleration. Negative values below -0.4 denote photospheric instability[8]. The hatched area is the region where the (downward) g_{eff} is overcompensated by the upward component of photospheric pulsational motions, which indicates stellar photospheric instability. A star like η Carinae apparently should have an unstable atmosphere, as appears from observations.

For blueward evolving stars, however, an interesting region appears, where the effective downward acceleration is strongly overcompensated by upward pulsational accelerations. In the Yellow Evolutionary Void the ratio reaches values down to -0.8 (= factor 6). We associate this void with the yellow hypergiants, and note here that ρ Cas is situated in the Hertzsprung-Russell diagram just at the low-temperature boundary of the void. This is less well the case for HR8752, which has still a distance to go, while HD33579 is situated in the middle of the region. That latter observation is in agreement with the fact (cf. Table I) the mass derived for HD33579 shows that this star has lost little mass and is evolving blueward.

We note that the void is also a region where strong mass loss can be expected in view of the fact that the stellar wind reaches sonic velocities already in photospheric layers. The lines in Fig. 7 connect points with the same values oflog$(v_{\text{wind}}/v_{\text{sound}})$. The hatched areas are the regions where $v_{\text{wind}} \geqslant v_s$. We remark that these areas coincide fairly well with the hatched areas in Fig. 6.

A possible explanation of the long-lasting hypergiant instabilities due to the large mass ejections now presents itself in a natural way : When a star, in its blueward evolution, approaches the void the photosphere becomes less stable, which results in a higher rate of mass loss. We advance the hypothesis that sudden large mass ejections may be associated with pulsational waves of large velocity amplitude and/or extension, causing a drastic increase of the rate of mass loss, presumably causing the ejection of an optically thick shell, which results in photospheric extension and therefore in smaller values for g_{eff} and T_{eff}.

Another region of instability occurs in the area of hotter more luminous very evolved stars and may be associated with Wolf-Rayet stars.

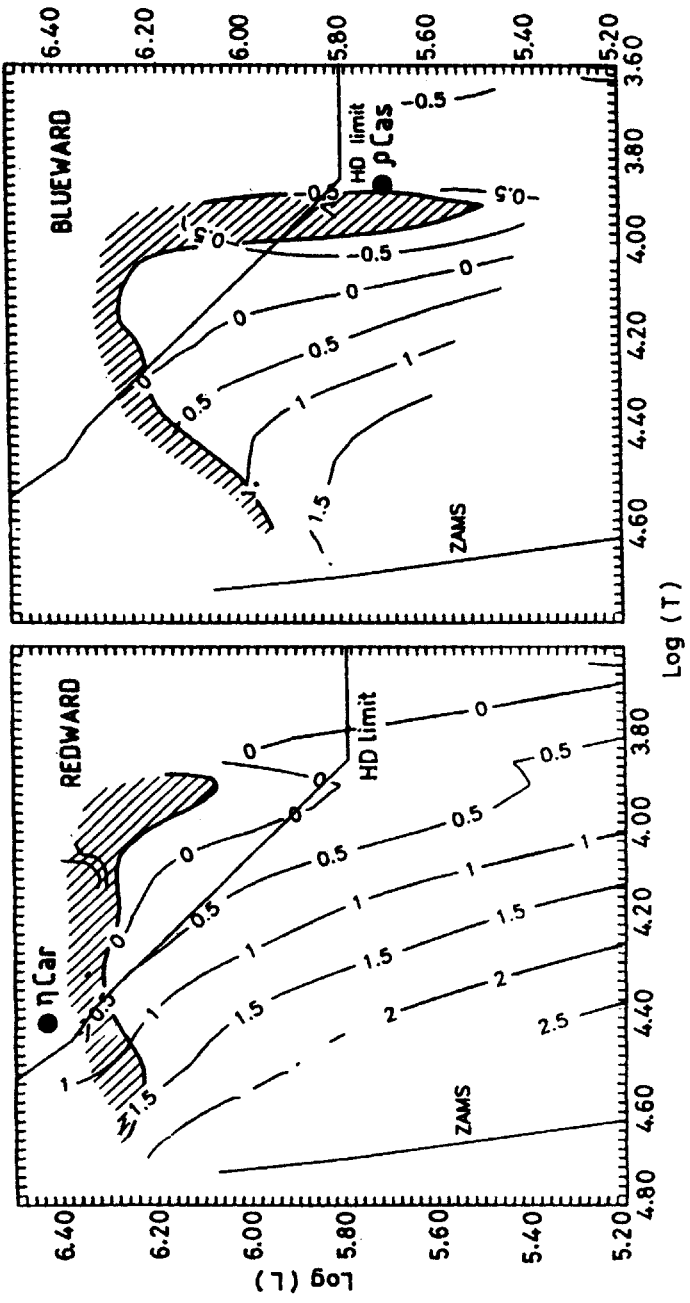

Fig. 7 Lines of equal log of ratio between wind and sound velocities over the HR diagram. *Left*: redward evolution; *right*: blueward. In hatched areas the wind velocity exceeds that of sound in photospheric layers

Conclusions

We think that the Yellow-white hypergiants exist because of the Void. They must be evolved stars—as is shown by the observations. Less evolved, still redward going stars like HD33579 have a larger mass at the same place of the HR diagram and are therefore more stable because of the larger values of the Newtonian gravitational attraction. The instability is made visible by mass expelled by pulsational motions and may in the most extreme case cause a significant reduction of the effective temperature and consequent change of spectral type. The motion field also contains a system of shock waves at mutual vertical distances smaller than 2.5 H_ρ.

Acknowledgement

Many thanks are due to Dr Arnout van Genderen and the coworkers Hans Nieuwenhuijzen and Alex Lobel for useful information and assistance in preparing this paper.

References

1 H Nieuwenhuijzen, C de Jager and H Groth *Submitted to Astron Astrophys* (1997)
2 H Nieuwenhuijzen, A Lobel and C de Jager *In prep.*, (*to be submitted to Astron Astrophys*) (1997)
3 A Lobel, L Achmad, C de Jager and H Nieuwenhuijzen *Astron Astrophys* **256** (1994) 159
4 H Nieuwenhuijzen and C de Jager *Paper presented at* 1995 *Liege Colloquium on Stellar Evolution* (1996)
5 A van Genderen *Astron Astrophys Suppl* **38** (1993) 151
6 —— *Astron Astrophys Suppl* **38** (1996) 381
7 L Achmad, C de Jager and H Nieuwenhuijzen *Astron Astrophys* **249** (1991) 192
8 H Nieuwenhuijzen and C de Jager *Astron Astrophys* **302** (1995) 811
9 C de Jager *Solar Phys* **25** (1991) 71
10 C de Jager and J Verma *Astrophys Space Sci* **26** (1979) 207
11 C de Jager, A de Koter, J Carpay and H Nieuwenhuijzen *Astron Astrophys* **244** (1991) 131
12 E A Spiegel *Astrophys J* **126** (1957) 202
13 C de Jager *The Brightest Stars* Reidel Dordrecht (1980)
14 C J Durrant *Astron Astrophys* **73** (1979) 137.
15 A Lobel, C de Jager, H Nieuwenhuijzen, J Smolinski and A Gesicki *Astron Astrophys* **291** (1994) 226
16 H Nieuwenhuijzen, C de Jager and M Cuntz *Astron Astrophys* **285** (1994) 595